Supplementary Materials to: Mixed diffusive/martensitic character of the pressure-induced $\beta \leftrightarrow \gamma$ transformation in tin

Robin Fréville[1,2,*], Agnès Dewaele[3,4], Charles Pépin[3,4], Nicolas Bruzy[3,4], Florent Occelli[3,4], Matteo Levantino[2], Nicolas Guignot[5]

[1] Karlsruhe Institute of Technology, Institute for Applied Materials, P.O. Box 3640, 76021 Karlsruhe, Germany

[2] European Synchrotron Radiation Facility, 71 Avenue des Martyrs, CS 40220, 38043 Grenoble, France

[3] CEA, DAM, DIF, F-91297 Arpajon, France

[4] Université Paris-Saclay, CEA, Laboratoire Matière en Conditions Extrêmes, 91680 Bruyères-le-Châtel, France

[5] Synchrotron Soleil, BP 48, 91192 Gif-sur-Yvette Cedex, France

[*] Corresponding author: robin.freville@esrf.fr

S.A. TWINNING ELEMENTS

Due to the reduced number of symmetries of β-Sn and γ-Sn compared to, e.g., cubic phases, twinning is likely to be frequently activated in these phases.

All twinning systems discussed in the text are reported in Table S1. For β-Sn, they have been observed directly [16, 48–50]. To our knowledge, γ-Sn being a high pressure phase, its twinning elements have not been measured. Indium has a crystal structure identical to γ-Sn: bct I4/mmm with $a = 4.60$ Å and $c = 4.95$ Å under ambient conditions; $(101)_\gamma$ twinning is described for this metal [50]. It can be seen as an exchange between $\vec{a}$ and $\vec{c}$ axes, producing a rotation of 85° around $\vec{b}$ axis. Another twinning system is described for bcc crystals, noted here $(112)_\gamma$; such deformation is also possible for bct crystals as noted in [16] and has been reported for bct steel [51].

Phase	**Structure**	**K1**	η_1	**K2**	η_2	**P**	Ref.	Misorientation	Noted
β-Sn	dbct I41/amd	(-301)	[103]	(101)	[-101]	(010)	[16, 48, 49]	62.8° around (010)	$(301)_\beta$
β-Sn	dbct I41/amd	(101)	[-101]	(-301)	[103]	(010)	[16, 48–50]	57.2° around (010)	$(101)_\beta$
γ-Sn	Bct I4/mmm	(101)	[10-1]	(-101)	[101]	(1-10)	[16, 50]	85° around (010)	$(101)_\gamma$
γ-Sn	Bct I4/mmm	(112)	[-1-11]	(11-2)	[111]	(1-10)	[16, 51]	68° around (1-10)	$(112)_\gamma$

TABLE S1: Possible twinning systems for β-Sn and γ-Sn. The twinning elements are as defined in Ref. [16]: K1 and K2 twinning and reciprocal planes; η_1 and η_2 twinning and reciprocal directions. P is the plane of shear.

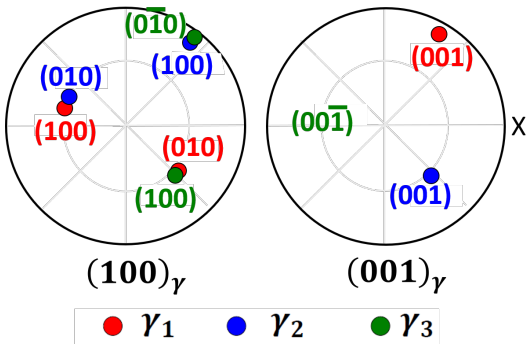

FIG. S1: Pole figure showing a clear twinning relationship between the three γ grains formed during Cycle 1, run 1. X is the compression axis.

S.B. CONDITIONS OF THE TRANSFORMATION AND EQUATION OF STATE

The β-Sn $\leftrightarrow$ γ-Sn transition pressures for all cycles of Runs 1 and 2 are reported in Table S2. For both runs, no β-Sn-γ-Sn coexistence domain was observed, with pressure steps of $\sim$0.2 GPa. This differs from one previous report where a β-Sn polycrystal was compressed: a β-Sn-γ-Sn coexistence domain was observed between 10.8 GPa and 15.6 GPa at 300 K [10]. Table S2 shows that transition pressures are all consistent for the direct β-Sn$\rightarrow$ γ-Sn transition, within $\pm$0.2 GPa. Interestingly, more scatter is observed for the reversion ($\pm$0.8 GPa).

Run, cycle	$P_{\beta\rightarrow\gamma}$ (GPa)	$P_{\gamma\rightarrow\beta}$ (GPa)	Ref.
Run 1, 1	10.7 $\pm$ 0.2	8.8 $\pm$ 0.1	TW
Run 1, 2	11.0 $\pm$ 0.1	8.7 $\pm$ 0.1	TW
Run 2, 1	10.9 $\pm$ 0.1	9.2 $\pm$ 0.3	TW
Run 2, 2	11.0 $\pm$ 0.3	9.8 $\pm$ 0.3	TW
Run 2, 3	10.9 $\pm$ 0.6	9.7 $\pm$ 0.6	TW
Run 2, 4	10.9 $\pm$ 0.2	10.2 $\pm$ 0.3	TW
Run 2, 5	11.1 $\pm$ 0.4		TW
	10.8 $\pm$ 4.8		[10]

TABLE S2: Pressures measured for the β-Sn$\leftrightarrow$bct-Sn transitions, for the grains followed in this study. $\pm$ indicate maximum coexistence domains. Data from ref. [10] (static hydrostatic loading) are included for comparison. TW: this work.

The P-V points collected during the two runs (compression and decompression) agree with the literature [10] as shown in the EOS displayed in Fig. S2. No drastic change in c_β/a_β or c_γ/a_γ was measured near the transitions. Here, c_β/a_β has a roughly constant value of 0.543; $c_\gamma/a_\gamma = 0.912$ at 11 GPa and increases with pressure as described in [10].

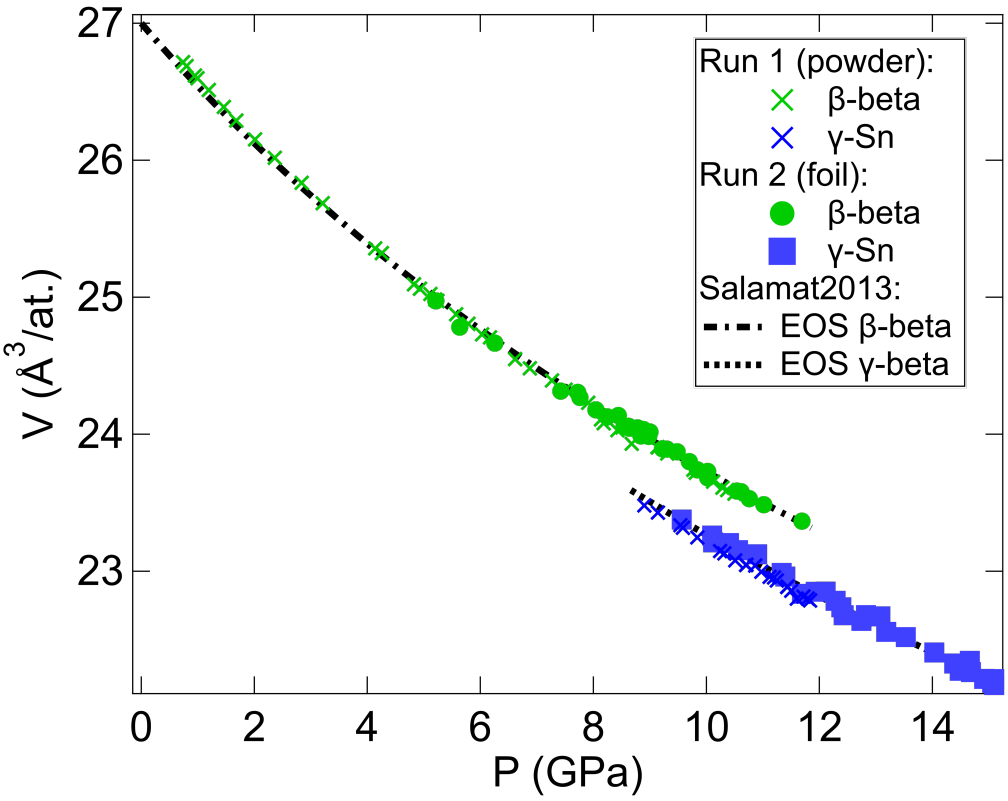

FIG. S2: Volume of β-Sn and γ-Sn measured on multiple compression/decompression cycles. EOS from Salamat et al. [10] are also plotted as dashed lines for comparison.

S.C. CRYSTAL QUALITY EVOLUTION WITH CYCLES

Fig. S3 shows an enlarged part of XRD images around one XRD peak during the experiment. It shows that the starting grain in Run 1 has a higher mosaicity than in Run 2, and the crystal healing after γ-Sn$\rightarrow$ β-Sn transition in Run 2.

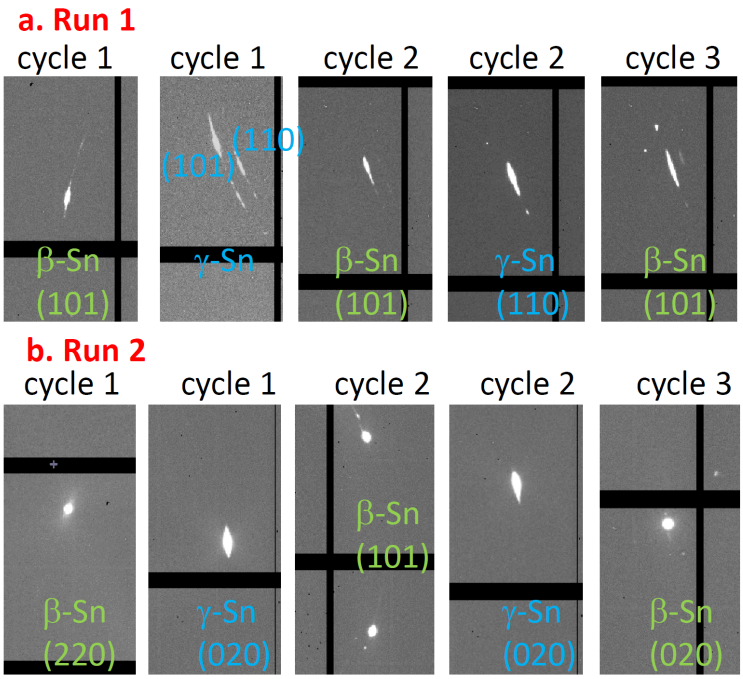

FIG. S3: Enlarged part of XRD images collected during Run 1 (a) and Run 2 (b). The starting grain in Run 1 had a high mosaicity ($\sim$3° FWHM extension in azimuthal angle χ), which further increased during the experiment ($\sim$4° FWHM in χ in cycle 3). For Run 2, an $\sim$1°/$\sim$3.5° FWHM extension is measured in β-Sn/γ-Sn for cycles 1-3.

S.D. EULER ANGLES AND ADDITIONAL POLE FIGURES

Table S3 reports Euler angles determined during our static experiment using a Bunge convention.

Run 1								Run 2							
	ϕ_1	Φ	ϕ_2		ϕ_1	Φ	ϕ_2		ϕ_1	Φ	ϕ_2		ϕ_1	Φ	ϕ_2
β_1	212.0°	77.5°	272.9°	γ_1	-134.2°	83.6°	-144.5°	β_A	-82.0°	84.4°	23.6°	γ_A	85.1°	20.8°	-9.0°
β_2	-168.2°	80.4°	-257.4°	γ_2	-49.0°	50.9°	81.5°	β_B	7.2°	269.9°	229.1°	γ_B	19.5°	304.3°	66.0°
β_2*	-111.8°	9.9°	18.6°	γ_3	-58.7°	143.1°	-185.1°	β_C	-3.0°	170.9°	176.9°	γ_C	15.2°	290.4°	129.3°
				γ_4	306.5°	52.4°	83.0°					γ_D	-66.1°	231.3°	-67.9°
				γ_5	111.3°	68.3°	294.3°					γ_{2A}	64.2°	264.0°	-13.9°
				γ_6	91.7°	132.5°	289.7°					γ_{2B}	-65.0°	70.7°	245.2°
				γ_5*	121.7°	71.4°	65.5°					γ_E	26.8°	97.8°	14.8°
												γ_F	-31.8°	247.9°	156.3°
												γ_G	28.9°	63.6°	61.8°
												γ_H	-29.3°	91.9°	74.8°

TABLE S3: Euler angles determined by XRD in this work. The three angles follow a Bunge convention. During run 1, * indicates the cycle at 425 K; Orientations differ due to the rotation induced when put in the oven.

These Euler angles can be used to plot pole figures of interest, such as the one displayed in the main text, or another example in Fig. S4, in the case of Run 1, cycle 2 and this work OR.

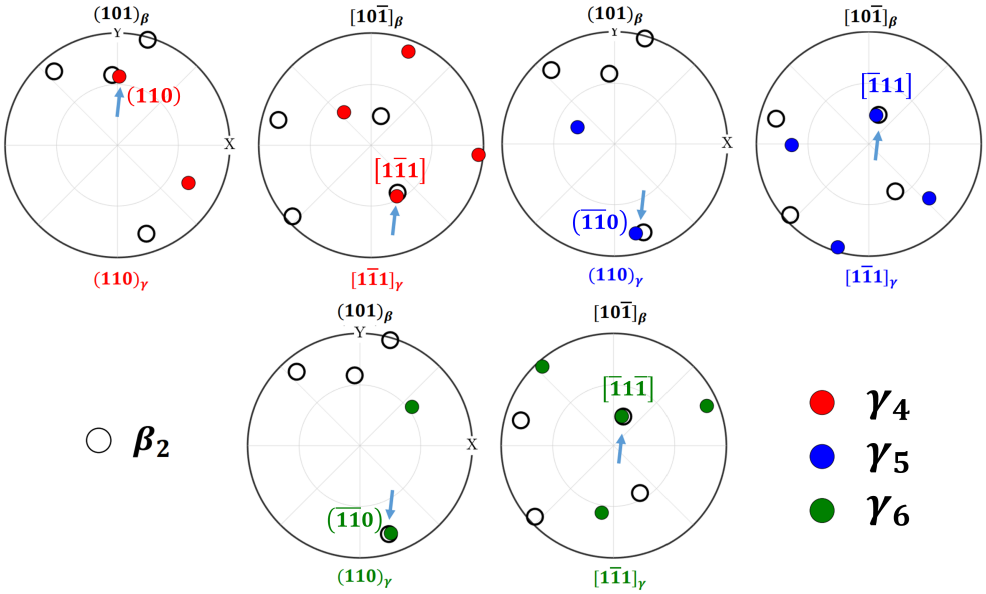

FIG. S4: Run 1, cycle 2: pole figures showing this work OR $((101)_\beta||(110)_\gamma$ and $[10\bar{1}]_\beta|||[1\bar{1}1]_\gamma)$ between β_2 (empty circle) and γ_4 (red circles), γ_5 (blue circles) and γ_6 (green circles). Arrows are visual guides to highlight the coincidences. The identification of plane and direction related to the mechanism are displayed for γ-Sn. X (horizontal) is the compression direction.

S.E. X-RAY SETUP AND RELEVANT ACQUISITION PARAMETERS

Experimental conditions for the 2 static experiments are summarized in Table S4, together with the relevant acquisition parameters used for multiexposure.

Run	sample form	P range (GPa)	θ_{max}	θ_{step}	Number of cycles	P gauge
1	powder grains	1-12	10°	1°	3	Au [35]
2	annealed foil	5-15	24°	1°	4.5	NaCl [36]

TABLE S4: Experimental conditions of Runs 1 and 2. One cycle corresponds to one experimental path in pressure that induced β-Sn$\rightarrow$ γ-Sn$\rightarrow$ β-Sn transformations. θ_{max} is the maximum rotation angle of the diamond anvil cell around a vertical axis used for the XRD data collection, and θ_{step} is its step used for the multiexposures.

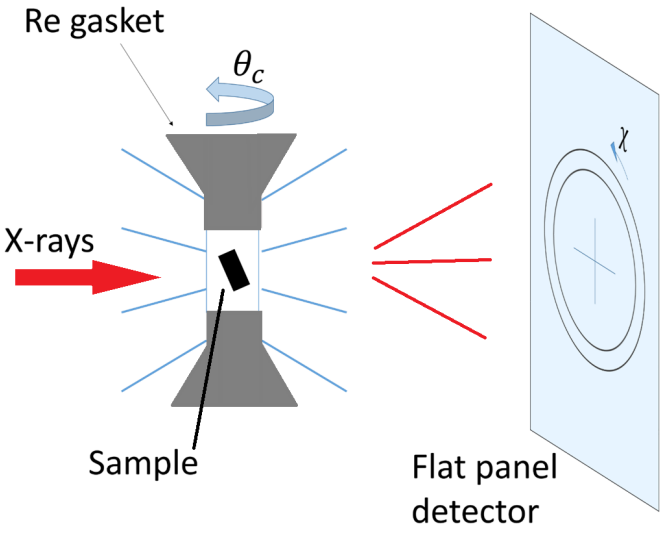

FIG. S5: Schematic representation of the X-ray diffraction setup used during the experiments.

S.F. VARIANTS CREATED BY THE PROPOSED MECHANISM

Planes	Directions	Variant name	Planes	Directions	Variant name
$(101)_\beta \|\| (110)_\gamma$	$[\bar{1}01]_\beta \|\| [\bar{1}11]_\gamma$	V.1	$(0\bar{1}1)_\beta \|\| (110)_\gamma$	$[011]_\beta \|\| [\bar{1}11]_\gamma$	V.5
	$[\bar{1}01]_\beta \|\| [1\bar{1}1]_\gamma$	V.2		$[011]_\beta \|\| [1\bar{1}1]_\gamma$	V.6
$(\bar{1}01)_\beta \|\| (110)_\gamma$	$[101]_\beta \|\| [\bar{1}11]_\gamma$	V.3	$(011)_\beta \|\| (110)_\gamma$	$[0\bar{1}1]_\beta \|\| [\bar{1}11]_\gamma$	V.7
	$[101]_\beta \|\| [1\bar{1}1]_\gamma$	V.4		$[0\bar{1}1]_\beta \|\| [1\bar{1}1]_\gamma$	V.8

TABLE S5: The eight possible variant of γ_{Sn} that can be produced starting from a single orientation of β_{Sn}, using the mechanism of this work.

S.G. COMPARISON BETWEEN MECHANISMS

Table S6 displays misorientation angles (in degrees) between measured orientations and theoretical orientations for runs 1 and 2, respectively. Theoretical orientations are associated with the transformation sequences given in the first two lines for several transitions reported in this work. These values were obtained using Vigilano software [52].

	TW	$(101)_\beta$+ $(101)_\beta$+K	$(301)_\beta$+ $(301)_\beta$+K	$(101)_\beta$+K +$(112)_\gamma$	$(301)_\beta$+ K+$(112)_\gamma$	K+$(112)_\gamma$ +$(112)_\gamma$	K+$(101)_\gamma$ +$(101)_\gamma$	$(301)_\beta$+K +$(101)_\gamma$	$(101)_\beta$+K +$(101)_\gamma$	K +$(101)_\gamma$	K +$(112)_\gamma$	$(301)_\beta$ +K	$(101)_\beta$ +K	K
$\beta_2 \leftarrow \gamma_2$	2.19	2.18	4.99	5.94	6.16	6.68	10.81	14.98	15.82	12.88	24.53	24.95	26.16	39
$\beta_2 \leftarrow \gamma_4$	2.4	2.23	3.91	4.38	4.87	5.57	10	16.05	16.94	12.51	24.18	24.67	26.03	40.24
$\beta_2 \leftarrow \gamma_5$	2.46	3.3	4.58	5.98	5.7	6.05	9.84	15.94	16.55	12.36	24.5	25	26.38	40.46
$\beta_2 \leftarrow \gamma_6$	0.79	2.19	2.76	4.3	3.95	4.47	11.5	14.55	15.34	14.14	22.66	23.13	24.48	40.49
$\beta_A \rightarrow \gamma_A$	1.91	3.81	3.97	6.24	5.2	5.25	11.32	14.67	15.1	13.99	23.1	23.6	24.99	40.93
$\beta_A \rightarrow \gamma_B$	1.26	3.26	2.43	4.85	3.68	3.86	12.96	13.23	13.89	15.69	21.23	21.7	23.02	40.82
$\beta_B \leftarrow \gamma_A$	5.33	6.73	4.34	6.29	4.64	4.41	9.73	18.08	18.64	13.51	22.02	22.66	24.34	44.66
$\beta_B \rightarrow \gamma_{2A}$	10.92	9.18	13.35	12.46	14.23	15.10	16.69	15.68	14.61	16.22	24.26	23.74	22.72	29.99
$\beta_B \rightarrow \gamma_{2B}$	1.22	1.17	3.65	4.51	4.77	5.41	12.34	13.67	14.68	14.61	22.74	23.14	24.31	39.2
$\beta_C \leftarrow \gamma_{2A}$	6.55	8.09	4.88	6.98	4.82	4.24	10.93	18.38	18.48	14.71	20.36	21.02	22.79	45.0
$\beta_C \leftarrow \gamma_{2B}$	6.69	8.61	6.25	9.18	6.74	5.88	17.42	10.82	10.48	20.47	17.2	17.68	19.10	40.79
$\beta_C \rightarrow \gamma_E$	1.4	1.65	2.76	3.63	3.81	4.54	12.46	13.82	14.84	14.95	22.09	22.52	23.77	39.89
$\beta_C \rightarrow \gamma_F$	1.24	1.86	3.82	4.98	5	5.53	11.06	14.79	15.62	13.44	23.59	24.04	25.32	39.78
$\beta_C \rightarrow \gamma_G$	3.07	4.18	3.76	5.61	4.67	4.82	15.1	11.1	11.96	17.63	19.87	20.24	21.36	39.95
$\beta_C \rightarrow \gamma_H$	2.81	4.27	3.26	5.29	4.21	4.36	10.1	16.25	16.72	13.24	23.22	23.81	25.37	42.23

TABLE S6: Misorientation angles (in degrees) between measured orientations and theoretical orientations associated with the transformation sequences given in the first two lines (the "+" symbol meaning a chaining of transformations within the sequence) for several transitions reported in this work. TW: transformation mechanism proposed in this work that produces $(101)_\beta||(110)_\gamma$ and $[10\bar{1}]_\beta||[1\bar{1}1]_\gamma$ OR. K: Katzke mechanism. The twins are defined in Table S1.

S.H. COMPUTATION OF THE TRANSFORMATION STRAIN

The transformation strain tensor explaining TW OR is computed in two steps. First, a shearing F_1 is evaluated so that atomic distances in $(101)_\beta$ planes after shuffle match those in γ-Sn. In particular, this plane contains the a axis of γ-Sn and a diagonal between a and b axes, denoted in the following as 'a/b diagonal'. Second, a second transformation F_2, leaving $(101)_\beta$ planes invariant, needs to restore normal distances according to γ-Sn dimensions and enforce the orthogonality between the two a/b diagonals. The total transformation is obtained by combining these two strains

Step 1

Let us consider, in the β-Sn cell after the shuffle described in Figure 4, the vectors $v_1 = [a_\beta, a_\beta, c_\beta]/2$ and $v_2 = [-a_\beta, a_\beta, c_\beta]/2$. They must become a vertical axis and an a/b diagonal of the γ-Sn cell after transformation, respectively. Let us work in the plane $(\tilde{X}, \tilde{Y})$ where X = $[0, a_\beta, 0]$, Y = $[a_\beta, 0, -c_\beta]$, and the tilde designates the normalization operator. In this basis, the transformation stretch U to be determined must verify:

$$\begin{cases} U.\begin{pmatrix} 0 \\ \sqrt{a_\beta^2 + c_\beta^2} \end{pmatrix} = \begin{pmatrix} 0 \\ \sqrt{2a_\gamma^2 + c_\gamma^2} \end{pmatrix} \\ U.\begin{pmatrix} \frac{a_\beta}{2} \\ \frac{\sqrt{a_\beta^2+c_\beta^2}}{2} \end{pmatrix} = \begin{pmatrix} \frac{\sqrt{2}a_\gamma c_\gamma}{\sqrt{2a_\gamma^2+c_\gamma^2}} \\ \frac{2a_\gamma^2}{\sqrt{2a_\gamma^2+c_\gamma^2}} \end{pmatrix} \end{cases} \tag{4}$$

After computation, one may obtain:

$$U = \begin{pmatrix} \frac{2\sqrt{2}a_\gamma c_\gamma}{a_\beta\sqrt{2a_\gamma^2+c_\gamma^2}} & 0 \\ \frac{2a_\gamma^2-c_\gamma^2}{a_\beta\sqrt{2a_\gamma^2+c_\gamma^2}} & \frac{\sqrt{2a_\gamma^2+c_\gamma^2}}{\sqrt{a_\beta^2+c_\beta^2}} \end{pmatrix} \tag{5}$$

The tensor F_1 in equation 7 is then obtained as:

$$F_1 = Q.\begin{pmatrix} U_{11} & U_{12} & 0 \\ U_{21} & U_{22} & 0 \\ 0 & 0 & 1 \end{pmatrix}.Q^T, \tag{6}$$

where T is the transpose operator and Q = $[\tilde{X}, \tilde{Y}, \tilde{X} \wedge \tilde{Y}]$.

For the following values: $a_\beta = 5.58$ Å and $c_\beta = 3.03$ Åand $a_\gamma = 3.694$ Å and $c_\gamma = 3.37$ Å, the shear strain is:

$$F_1 = \begin{bmatrix} 0.984 & 0.404 & 0.009 \\ 0. & 1.015 & 0. \\ 0.009 & -0.219 & 0.995 \end{bmatrix} . \tag{7}$$

Step 2

Let us now consider $v_3 = [-a_\beta, a_\beta, -3c_\beta]/2$. This vector becomes the other a/b diagonal of the γ-Sn cell after transformation. It will then be orthogonal to the transformed $(101)_\beta$ plane. Let n be the normal to this plane. v_3 is decomposed as follows: $v_3 = (v_3.n)n + d.m$ with m a normalized vector. The tensor F_2 is then obtained as:

$$F_2 = I + \frac{\sqrt{2}a_\gamma - v_3.n}{v_3.n} n \otimes n + \frac{d}{v_3.n} m \otimes n, \tag{8}$$

with I the identity of second-order tensors.

After calculation, its components are such that:

$$F_2 = \begin{bmatrix} 1.075 & 0. & 0.138 \\ 0.254 & 1. & 0.467 \\ -0.051 & 0. & 0.906 \end{bmatrix} . \tag{9}$$

The total transformation is obtained by combining these two strains:

$$F = F_2.F_1 = \begin{bmatrix} 1.06 & 0.40 & 0.15 \\ 0.25 & 1.02 & 0.47 \\ -0.04 & -0.22 & 0.90 \end{bmatrix} . \tag{10}$$

Once this transformation strain is known, it can be applied to a group of shuffled β-Sn cells to find three vectors with norms a_γ, a_γ and c_γ forming a direct orthonormal basis. The corresponding rotation matrix from β-Sn to γ-Sn lattice is:

$$\mathcal{R} = \begin{bmatrix} -0.18 & 0.86 & -0.48 \\ -0.38 & 0.38 & 0.84 \\ 0.90 & 0.34 & 0.26 \end{bmatrix} . \tag{11}$$

It can be easily verified that the rotation $\mathcal{R}$ permits verifying the observed OR: $(101)_\beta||(110)_\gamma$ and $[10\bar{1}]_\beta||[1\bar{1}1]_\gamma$.